

# RRA-U-Net: A RESIDUAL ENCODER TO ATTENTION DECODER BY RESIDUAL CONNECTIONS FRAMEWORK FOR SPINE SEGMENTATION UNDER NOISY LABELS

Ziyang Wang<sup>1</sup>, Zhengdong Zhang<sup>2</sup>, Irina Voiculescu<sup>1</sup>

<sup>1</sup>Department of Computer Science, University of Oxford, UK

<sup>2</sup> Beihang University, Beijing, China

## ABSTRACT

Segmentation algorithms of medical image volumes are widely studied for many clinical and research purposes. We propose a novel and efficient framework for medical image segmentation. The framework functions under a deep learning paradigm, incorporating four novel contributions. Firstly, a residual interconnection is explored in different scale encoders. Secondly, four copy and crop connections are replaced to residual-block-based concatenation to alleviate the disparity between encoders and decoders, respectively. Thirdly, convolutional attention modules for feature refinement are studied on all scale decoders. Finally, an adaptive clean noisy label learning strategy(ACNLL) based on the training process from underfitting to overfitting is studied. Experimental results are illustrated on a publicly available benchmark database of spine CTs. Our segmentation framework achieves competitive performance with other state-of-the-art methods over a variety of different evaluation measures.

**Index Terms**— Semantic Segmentation, Computed Tomography, U-Net, Spine

## 1. INTRODUCTION

As machine learning technologies, especially deep learning, studied in medical image analysis, convolutional neural networks shows its robust state-of-the-art performance in medical image segmentation. Encoder-Decoder architecture has been one of the most prominent deep neural networks in the biomedical image segmentation area. U-Net, a completely symmetric encoder-decoder architecture for biomedical image segmentation, was first proposed by Ronneberger [1]. The encoder is to extract pixel location features with down sampling, and the decoder is to recover the spatial dimension and pixel location features with deconvolution. A copy and crop connection is between the corresponding encoder and decoder layers respectively. Meanwhile, U-Net shows increasingly promising results in biomedical image segmentation vary from brain, spine, lung and other areas of interest. Martin came up an optimized high resolution 2D Dense-U-Net Network for spine segmentation in 2019[2]. His study

explores the performance of 2D and 3D U-Net with several cut-of-edge techniques such as residual networks and densely connected networks, respectively. The 3D convolutional layers and interconnections, however, lead to the training parameters or computational cost been significantly increased. Semi-supervised learning or training under noisy label can also be potentially studied.

Following the above consideration, a novel encoder-decoder architecture for medical image segmentation is proposed. Firstly, inspired by ResNet shows promising results taking into account the computation resources available [3], shortcut interconnections are explored on four down-sampling blocks as residual encoders. Secondly, instead of four copy and crop connections utilized encoders to decoders, a residual-block-based concatenation is proposed to alleviate the disparity with easier learning task for optimizer. Thirdly, convolutional attention module is explored on four up-sampling blocks. It aims to increase weight of feature map on important features and suppressing unnecessary area and noisy label. In the end, an adaptive learning approach is proposed to avoid noisy label under practical clinical environment. The adaptive learning approach allows clean noisy label while training process. RRA-U-Net is tested, compared with other classical models, with ablation studies, and evaluated with a large collection of metrics. The results achieve competitive performance compared with other state-of-the-art approaches.

## 2. METHODS

The residual encoder to attention decoder by residual connections framework is illustrated in Figure 1. The proposed framework utilizes encoder-decoder architecture as the backbone. A symmetrical architecture which consists of convolutional, deconvolutional, upsampling, and downsampling allows to contract and recover pixel-level information. The contribution consists of four components: residual shortcut connection in encoder, residual block based connection, attention decoder, and the adaptive clean noisy label learning strategy(ACCLL). They are studied and discussed in the section 2.1, 2.2, 2.3, and 2.4, respectively.

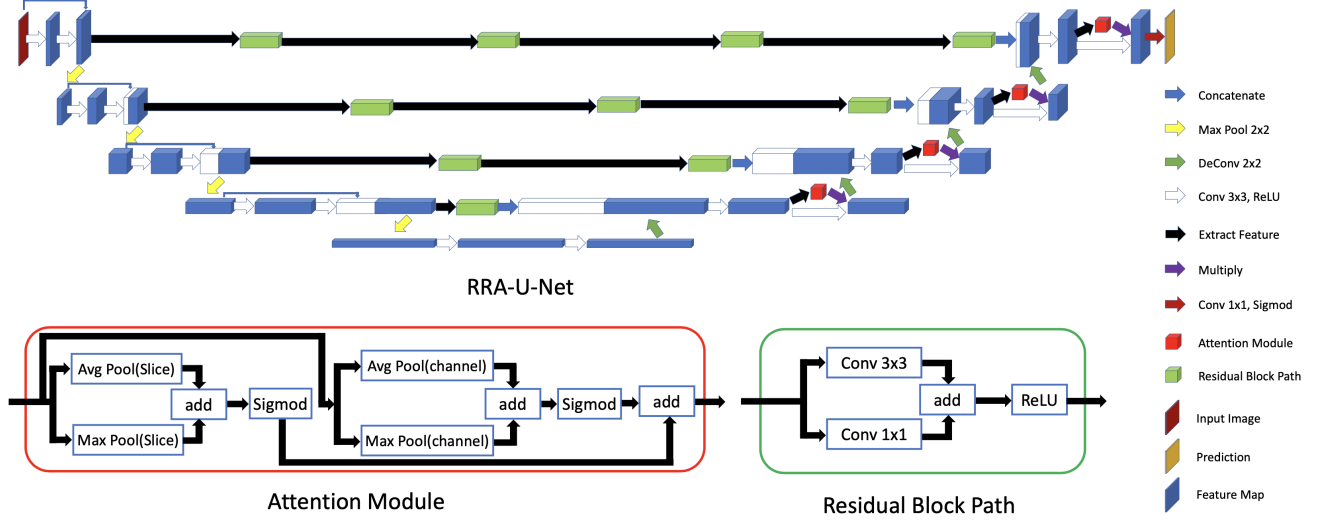


Fig. 1: The Architecture of the Proposed RRA-U-Net Network, Attention Module and Residual Block Path

## 2.1. Residual Interconnections Networks

Inspired by ResNet [3], a concatenation function is designed in each down-sampling block. In order to strengthen the ability to express features, after obtaining the down-sampled features of the previous layer, these features will go through a new feature extraction process. The extraction process consists of the repeated application of two 3x3 convolutions (unpadded convolutions), each followed by a rectified linear unit (ReLU). The number of feature channels is doubled compared with previous layer after the first 3x3 convolution operator. At last, we concatenate the down-sampled feature with the feature acquired from the second 3x3 convolution operator. This operation aims at establishing connections between different layers, making full use of feature information and alleviating the problem of gradient disappearance to a certain extent.

## 2.2. Residual-Block-Based Connection Paths

Considering the disparity between encoders and decoders which may degrade the segmentation performance [4]. The four copy and crop connections are replaced by residual-block-based concatenation to alleviate the disparity between encoders and decoders in each layer, respectively. We adopt residual learning to connect encoder to decoder in each layer. A building block is shown in Fig. 1 which is named as Residual Block Path. Formally, in this paper we define a building block in Equation 1.

$$y = F(x, \{W_i\}) + x \quad (1)$$

Here  $x$  and  $y$  are the input and output vectors of the layers considered. The function  $F(x, \{W_i\})$  represents the residual

mapping to be learned. For the example in Fig. 1 that has one 3x3 layer,  $F = \sigma W_1 x$  in which  $\sigma$  denotes ReLU and the biases are omitted for simplifying notations. The operation  $F + x$  is performed by a shortcut connection and element-wise addition. In addition, we use 1x1 convolution operator to match the number of channels. Then, We adopt the second non-linearity ReLU after the addition operation. Finally, the processed feature map through residual block is concatenated with upsampled feature of the decoder. The number of Residual Blocks in each level of Encoder-Decoder is 4, 3, 2 and 1, respectively.

## 2.3. Convolutional Attention Module

To enhance the decoder performance of classification for each pixel under noisy label, attention mechanism is explored. Unlike attention gate filter features from skip connection [5], attention module can normally be integrated with convolutional layers to enhance key information on feature map with pooling layers and sigmoid activation functions [6]. In this proposed attention module for convolutional layer of decoder, two attention parts including channel and slice of each feature map are studied, respectively. Both of attention parts developed by pooling layer and sigmoid activation. Average and max pooling layers avoid noisy label gradients to update trunk parameters. Sigmoid allow the output is the weight attention value for each pixel location. As shown in Figure 1, a feature map  $F \in R^{W \times H \times D}$  from previous CNN is sent to attention module pipeline.  $F_{Slice}^{Avg}, F_{Slice}^{Max} \in R^{W \times H \times 1}$  are the feature maps from average pooling layers and max pooling layers on the dimension of slice.  $F_{Channel}^{Avg}, F_{Channel}^{Max} \in R^{1 \times 1 \times D}$  are the feature maps from average pooling layers and max pooling layers on the dimension of channel. The final output of

weight attention value  $W$  is calculated by above feature maps illustrated in Equation 2, where  $\sigma$  is Sigmod activation, and then can be multiplied with provided features.

$$W = \sigma(F_{Slice}^{Avg} + F_{Slice}^{Max}) + \sigma(F_{Channel}^{Avg} + F_{Channel}^{Max}) \quad (2)$$

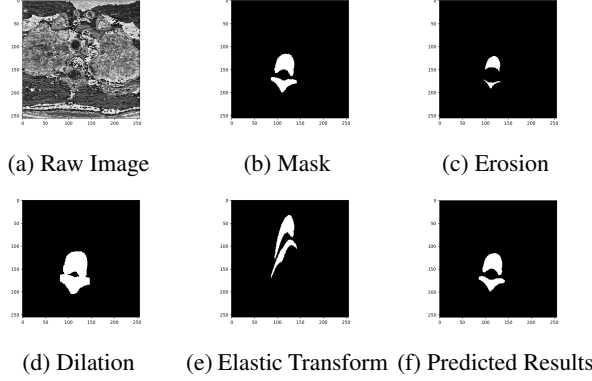


Fig. 2: CT Spine Slice Examples

#### 2.4. Adaptive Clean Noisy Label Learning

Deep learning training in clinical environment are suffering from the problem of inaccuracy labeled data. Different operators can label a same CT scan with different masks or even result in wrong label as noisy label. To deal with this realistic challenge, ACNLL in training process is proposed. Masks in the training dataset are randomly selected and manually replaced as noisy labels. They are created by erosion, dilation and elastic transform, and three noisy label examples are illustrated in Figure 2c, 2d, 2e. Two parameters for noisy dataset including: a) the noisy level of noisy label  $\alpha \in (0, 1)$ , b) the proportion of noisy label  $\beta$  are both defined and test in this experiment. The noisy level  $\alpha$  is the dice coefficient between the original training dataset and noisy label dataset. Different from detecting and cleaning noisy label before training, a simple and efficient adaptive clean noisy label learning method is proposed. Inspired by O2U-Net [7], the losses of each label are recorded while training, and the higher of loss of a label, the higher probability of being noisy label. The proposed ACNLL allows to clean a specific number of label with high loss value during iteration. A large number of noisy labels are detected intuitively at the beginning of iteration, and then few number of noisy label at the end, because training model is a kind of process from underfitting to overfitting. The number of labels detected and removed for each epoch is illustrated as Noisy Label  $N(t)$  follow the rule:

$$N(t) = \begin{cases} 0.5(1 - \alpha)\beta y t, & t < 0.1(1 - \alpha)\beta y \\ \frac{y}{x} t, & 0.1(1 - \alpha)\beta y \leq t < 0.5(1 - \alpha)\beta y \\ 0.1(1 - \alpha)\beta y t, & t \geq 0.5(1 - \alpha)\beta y \end{cases} \quad (3)$$

Table 1: Segmentation Results on Spine CT Dataset

Model	Dice	Acc	Pre	Rec	Spe
UNet	0.8360	0.9863	0.8832	0.7936	0.9952
Residual-UNet	0.8810	0.9898	0.9097	0.8540	0.9961
Densely-UNet	0.8316	0.9860	0.8832	0.7857	0.9952
M-UNet	0.9478	0.9954	0.9512	0.9444	0.9978
M-Densely-UNet	0.9517	0.9958	0.9524	0.9508	0.9978
VGG16 UNet	0.9138	0.9925	0.9235	0.9043	0.9966
ResNet34 UNet	0.6626	0.9689	0.6333	0.6947	0.9815
SE-ResNet34 UNet	0.7306	0.9762	0.7265	0.7347	0.9873
ResNeXt101 UNet	0.7597	0.9765	0.6909	0.8438	0.9826
DenseNet121 UNet	0.7982	0.9811	0.7526	0.8498	0.9872
InceptionV3 UNet	0.8109	0.9837	0.8250	0.7972	0.9922
EfficientNet UNet	0.8358	0.9857	0.8431	0.8286	0.9929
MultiRes UNet	0.8542	0.9864	0.8094	0.9043	0.9902
LinkNet	0.8958	0.9908	0.8919	0.8999	0.9950
FPN	0.8804	0.9893	0.8675	0.8936	0.9937
<b>RRA-UNet</b>	<b>0.9580</b>	<b>0.9963</b>	<b>0.9605</b>	<b>0.9554</b>	<b>0.9982</b>

Table 2: Boundary-based Segmentation Results

	BoundaryGT	BoundaryMS	BoundarySymmetric
Dice	0.8425	0.8564	0.8465
TPVF	0.8274	0.8636	0.8420
TNVF	0.7824	0.6754	0.7298
FPVF	0.2176	0.3245	0.2702
FNVF	0.1726	0.1364	0.1579

where  $t$  is the training progress illustrated by training epoch,  $\alpha$  is the noise level of training masks,  $\beta$  is the proportion of noisy label in training dataset,  $x$  is the total number of training epochs, and  $y$  is the total number of masks.

### 3. EXPERIMENTS AND RESULTS

#### 3.1. Dataset

Spine dataset is provided by the University of California and National Institutes of Health [8]. It consists of CT scans from 10 patients, of up to 600 slices per scan, at a resolution of  $512 \times 512$ , and an inter-slice spacing of 1mm. In our study, all images are normalized and resized to  $256 \times 256$ . Then, the associated ground truth (GT) comes with a semantic binary segmentation where any spine tissue is assigned a value of 1, whereas the rest is labelled as 0. Finally, 90 degree rotation is applied for U-Net and all other extended frameworks. Of the 10 scans, 9 were used for training and 1 for testing. Validation is carried out on 10% of the training data.

#### 3.2. Experimental Setup

RRA-U-Net is developed in Python using Tensorflow. It has been run under Ubuntu 18.04.1 on an Nvidia GeForce

RTX2080 Ti GPU with 16GB memory, and Intel(R) Xeon(R) CPU E5-2650 v4. Runtimes varied between 1000 and 1200 minutes of overall CPU time. With a training batch size of 8, the learning rate is  $10^{-5}$ . Rather than accuracy, dice coefficient is selected as loss function, because of the imbalance between background and spine. The training epochs setting is illustrated in Section 2.4. Some of the benchmarks are developed by an open source library [9].

### 3.3. Results and Discussion

Fig. 2a, 2b, and 2f illustrate an example raw image, GT mask and predicted result. To evaluate the performance, we have assessed our predicted masks against the GT masks available with the dataset. The performance of our algorithm is compared against a collection of other algorithms. A high score in the generic class of Overlap Measures (Dice coefficient, Specificity, Recall, Precision, Accuracy) ensuring a reliable volumetric calculation are illustrated in Table 1. Not only overlap measures, but also extended measures [10] are used for segmentation evaluation. A family of boundary match measures are defined, and some of which we report here under the names Directed Boundary Dice relative to GT ( $DBD_G$ ), Directed Boundary Dice relative to MS ( $DBD_M$ ) and Symmetric Boundary Dice (SBD). These measures penalise mislabelled areas in the machine segmentation. In this case, a 50% match between the boundaries is considered a good result. Seen that the boundary match is an asymmetric (directional) measure,  $DBD_M$  (0.8564) is invariably better. In Table 2 we report all three kinds of boundary-based measures. Extensive ablation experiments are also conducted to analyze the effects of four proposed contributions and their combinations. The results are documented in Table 3 and Table 4, four proposed contributions can significantly improve the segmentation performance in individual cases.

## 4. CONCLUSIONS

In this study, a framework for medical image segmentation is proposed and studied. Comprehensive evaluations and comparisons are completed, and RRA-U-Net achieves

**Table 3:** Ablation Studies on Contributions of Architecture

Residual Encoders	Residual Connections	Spatial Attention Decoders	Dice	Acc
			0.8360	0.9863
✓			0.9489	0.9954
	✓		0.9539	0.9960
		✓	0.9433	0.9950
✓		✓	0.9513	0.9957
✓	✓		0.9543	0.9960
✓	✓	✓	<b>0.9580</b>	<b>0.9963</b>

**Table 4:** Ablation Studies on ACNLL

Proportion	Level	Algorithm	ACNLL	Dice	Acc
75%	0.68	2D-U-Net		0.7838	0.9823
75%	0.68	2D-U-Net	✓	<b>0.8054</b>	<b>0.9929</b>
75%	0.68	2D-Residual-UNet		0.8699	0.9882
75%	0.68	2D-Residual-UNet	✓	<b>0.8769</b>	<b>0.9889</b>
75%	0.68	RRA-UNet		0.9314	0.9939
75%	0.68	RRA-UNet	✓	<b>0.9380</b>	<b>0.9945</b>
50%	0.77	2D-U-Net		0.9202	0.9929
50%	0.77	2D-U-Net	✓	<b>0.9206</b>	<b>0.9930</b>
50%	0.77	2D-Residual-UNet		0.9012	0.9913
50%	0.77	2D-Residual-UNet	✓	<b>0.9327</b>	<b>0.9941</b>
25%	0.85	2D-U-Net		0.9268	0.9937
25%	0.85	2D-U-Net	✓	<b>0.9284</b>	<b>0.9938</b>
25%	0.55	2D-U-Net		0.8904	0.9901
25%	0.55	2D-U-Net	✓	<b>0.9073</b>	<b>0.9919</b>
25%	0.55	2D-Residual-UNet		0.9029	0.9915
25%	0.55	2D-Residual-UNet	✓	<b>0.9186</b>	<b>0.9929</b>

promising performance. In the future, semi-supervised learning based on RRA-U-Net with unlabeled data will be studied.

## 5. REFERENCES

- [1] O Ronneberger et al., “U-net: Convolutional networks for biomedical image segmentation,” in *Int Conf Med Im Comp & Comp-Assisted Intervention*. Springer, 2015, pp. 234–241.
- [2] M Kolařík et al, “Optimized high resolution 3d dense-u-net network for brain and spine segmentation,” *Applied Sciences*, vol. 9, no. 3, pp. 404, 2019.
- [3] K He et al, “Deep residual learning for image recognition,” in *Proc IEEE CVPR*, 2016, pp. 770–778.
- [4] Nabil Ibtchaz and M Sohel Rahman, “Multiresunet: Rethinking the u-net architecture for multimodal biomedical image segmentation,” *Neural Networks*, vol. 121, pp. 74–87, 2020.
- [5] O Oktay et al., “Attention u-net: Learning where to look for the pancreas,” *arXiv preprint arXiv:1804.03999*, 2018.
- [6] S Woo et al., “Cbam: Convolutional block attention module,” in *Proc ECCV*, 2018, pp. 3–19.
- [7] J Huang et al., “O2u-net: A simple noisy label detection approach for deep neural networks,” in *Proc IEEE ICCV*, 2019, pp. 3326–3334.
- [8] J Yao et al, “Detection of vertebral body fractures based on cortical shell unwrapping,” in *Int Conf Med Im Comp & Comp-Assisted Intervention*. Springer, 2012, pp. 509–516.
- [9] Pavel Yakubovskiy, “Segmentation models,” [https://github.com/qubvel/segmentation\\_models](https://github.com/qubvel/segmentation_models), 2019.
- [10] V Yeghiazaryan et al., “Family of boundary overlap metrics for the evaluation of medical image segmentation,” *SPIE JMI*, vol. 5, no. 1, pp. 015006, 2018.